An X-ray Study of the Effect of the Bite Angle of Chelating Ligands on the Geometry of Palladium(allyl) Complexes: Implications for the Regioselectivity in the Allylic Alkylation

Richard J. van Haaren,[†] Kees Goubitz,[†] Jan Fraanje,[†] Gino P. F. van Strijdonck,[†] Henk Oevering,[‡] Betty Coussens,[‡] Joost N. H. Reek,[†] Paul C. J. Kamer,[†] and Piet W. N. M. van Leeuwen*,[†]

Institute of Molecular Chemistry, University of Amsterdam, Nieuwe Achtergracht 166, 1018 WV, Amsterdam, The Netherlands, and DSM Research B.V., Postbus 18, 6160 MD, Geleen, The Netherlands

Received August 11, 2000

X-ray crystal structures of a series of cationic (P-P)palladium(1,1-$(CH_3)_2C_3H_3$) complexes (P-P = dppe (1,2-bis(diphenylphosphino)ethane), dppf (1,1′-bis(diphenylphosphino)ferrocene), and DPEphos (2,2′-bis(diphenylphosphino)diphenyl ether)) and the (Xantphos)Pd(C_3H_5)BF_4 (Xantphos = 4,5-bis(diphenylphosphino)-9,9-dimethylxanthene) complex have been determined. In the solid state structure, the phenyl rings of the ligand are oriented in the direction of the nonsymmetrically bound [1,1-$(CH_3)_2C_3H_3$] moiety. An increase of the bite angle of the chelating ligand results in an increase of the cone angle. In complexes containing ligands having a large cone angle, the distances between the phenyl rings and the allyl moiety become small, resulting in a distortion of the symmetry of the palladium−allyl bond. In solution, two types of dynamic exchange have been observed, the $\pi-\sigma$ rearrangement and the apparent rotation of the allyl moiety. At the same time, the folded structure of the ligand changes from an endo to an exo orientation or vice versa. The regioselectivity in the palladium-catalyzed allylic alkylation of 3-methyl-but-2-enyl acetate is determined by the cone angle of the bidentate phosphine ligand. Nucleophilic attack by a malonate anion takes place preferentially at the allylic carbon atom having the largest distance to palladium. Ligands with a larger cone angle direct the regioselectivity to the formation of the branched product, from 8% for dppe (**1**) to 61% found for Xantphos (**6**). The influence of the cone angle on the regioselectivity has been assigned to a sterically induced electronic effect.

Introduction

In many cases, palladium is the metal of choice in the synthetically useful allylic alkylation reaction.[1] When substrates giving symmetrically substituted Pd(allyl) complexes are used, such as cyclopent-2-enyl acetate or 1,3-diphenylprop-2-enyl 1-acetate, high enantioselectivities can be obtained.[2−4] The ligands that can be employed range from monodentate phosphorus ligands to bidentate phosphorus,[2] nitrogen,[3] or mixed bidentate P-N, P-S, or phosphine-phosphite ligands.[4]

When other types of allylic substrates are used, such as crotyl acetate or cinnamyl acetate, nonsymmetrically substituted Pd(allyl) complexes are formed and regiocontrol[5] becomes an issue prior to enantiocontrol (see Scheme 1). Three products can be formed: the nonchiral *E* and *Z* linear products and the chiral branched product. Excellent regio- and enantioselectivities have been obtained using P−N ligands with palladium as the metal.[6] The use of other metals, such as iridium,[7a−d] rhodium,[7e] or tungsten,[7h] can lead to analogous results, although the reaction rates are lower than those employing palladium. At this time, palladium-based systems are still the most widely studied.

Although many papers have appeared on enantioselective allylic alkylation, the subject of regioselectivity is studied less extensively. When a bidentate P-N or P-S ligand is used, the

* Corresponding author.
† University of Amsterdam.
‡ DSM Research B.V.

(1) Trost, B. M.; van Vranken, D. V. *Chem. Rev.* **1996**, *96*, 395−422.
(2) (a) Dierkes, P.; Ramdeehul, S.; Barloy, L.; de Cian, A.; Fischer, J.; Kamer, P. C. J.; van Leeuwen, P. W. N. M.; Osborn, J. A. *Angew. Chem., Int. Ed.* **1998**, *37*, 3116−3118. (b) Fuji, K.; Kinoshita, N.; Tanaka, K. *Chem. Commun.* **1999**, 1895−1896.
(3) Svensson, M.; Bremberg, U.; Hallmann, K.; Csoregh, I.; Moberg, C. *Organometallics* **1999**, *18*, 4900−4907. Pfaltz, A. *Acc. Chem. Res.* **1993**, *26*, 339−345.
(4) (a) Helmchen, G. *J. Organomet. Chem.* **1999**, *576*, 203-214 and references therein. (b) Selvakumar, K.; Valentini, M.; Worle, M.; Pregosin, P. S.; Albinati, A. *Organometallics* **1999**, *18*, 1207−1215. (c) von Matt, P.; Lloyd-Jones, G. C.; Minidis, A. B. F.; Pfaltz, A.; Macko, L.; Neuburger, M.; Zehnder, M.; Ruegger, H.; Pregosin, P. S. *Helv. Chim. Acta* **1995**, *78*, 265−284. (d) Albinati, A.; Pregosin, P. S.; Wick, K. *Organometallics* **1996**, *15*, 2419−2421. (e) Yonehara, K.; Hashizume, T.; Mori, K.; Ohe, K.; Uemura, S. *Chem. Commun.* **1999**, 415−416.
(5) (a) Hayashi, T.; Kawatsura, M.; Uozomi, Y. *J. Am. Chem. Soc.* **1998**, *120*, 1681−1687. (b) Sjogren, M. P. T.; Hansson, S.; Åkermark, B.; Vitagliano, A. *Organometallics* **1994**, *13*, 1963−1971. (c) Kranenburg, M.; Kamer, P. C. J.; van Leeuwen, P. W. N. M. *Eur. J. Inorg. Chem.* **1998**, 25−27. (d) Blacker, A. J.; Clarke, M. L.; Loft, M. S.; Williams, J. M. J. *Org. Lett.* **1999**, *1*, 1969−1971. (e) Keinan, E.; Sahai, M. *J. Chem. Soc., Chem. Commun.* **1984**, 648−650. (f) Oosterom, G. E.; Van Haaren, R. J.; Reek, J. N. H.; Kamer, P. C. J.; Van Leeuwen, P. W. N. M. *Chem. Commun.* **1999**, 1119−1120.
(6) (a) Pretot, R.; Pfaltz, A. *Angew. Chem., Int. Ed.* **1998**, *37*, 323−325. (b) Vyskocil, S.; Smrcina, M.; Hanus, V.; Polasek, M.; Kocovsky, P. *J. Org. Chem.* **1998**, *63*, 7738−7748.
(7) (a) Iridium: Takeuchi, R.; Kashio, M. *J. Am. Chem. Soc.* **1998**, *120*, 8647−8655. (b) Bartels, B.; Helmchen, G. *Chem. Commun.* **1999**, 741−742. (c) Fuji, K.; Kinoshita, N.; Tanaka, K.; Kawabata, T. *Chem. Commun.* **1999**, 2289−2290. Molybdenum: (d) Sjogren, M. P. T.; Frisell, H.; Åkermark, B.; Norrby, P.-O.; Eriksson, L.; Vitagliano, A. *Organometallics* **1997**, *16*, 942−950. Rhodium: (e) Evans, P. A.; Nelson, J. D. *J. Am. Chem. Soc.* **1998**, *120*, 5581−5582. Platinum: (f) Blacker, A. J.; Clark, M. L.; Loft, M. S.; Williams, J. M. J. *Chem. Commun.* **1999**, 913−914. (g) Blacker, A. J.; Clarke, M. L.; Loft, M. S.; Mahon, M. F.; Humphries, M. E.; Williams, J. M. J. *Chem.—Eur. J.* **2000**, *6*, 353−360. Tungsten: (h) Pretot, R.; Lloyd-Jones, G. C.; Pfaltz, A. *Pure Appl. Chem.* **1998**, *70*, 1035−1040.

10.1021/ic0009167 CCC: $20.00
Published on Web 06/07/2001

Scheme 1. Regioselectivity in the Palladium-Catalyzed Allylic Alkylation

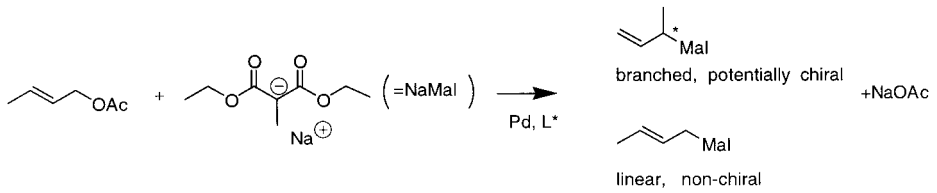

Scheme 2. Distorted Coordination of a Substituted Allyl Moiety to Palladium

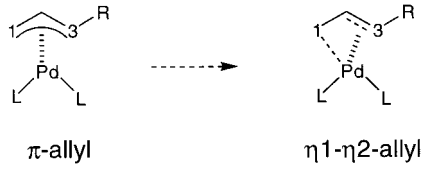

regioselectivity is determined by the difference in trans influence of the ligand donor atoms. The nucleophilic attack consequently takes place trans to the phosphorus donor, which in many cases exerts the strongest trans influence.[8]

For complexes containing bidentate P-P or N-N ligands, it has been suggested that the regioselectivity is determined by the bonding of the allyl moiety.[9] When the allyl group is substituted at one of its terminal positions, the symmetry of its bond to palladium is disturbed. QSAR studies by Åkermark[9a] show that the Pd−allyl bond is distorted from an η^3 to an η^1,η^2-like structure (see Scheme 2). The Pd−C1 bond is shorter than the Pd−C3 bond, and, at the same time, the C1−C2 bond is elongated and the C2−C3 bond is shortened. In literature many examples are known of crystal structures of substituted allyl moieties that are not symmetrically bonded to palladium.[10] On the basis of NMR studies, it has been suggested that the electrophilicity of the substituted allylic carbon atom site is enhanced relative to the nonsubstituted terminal site. It appears that the malonate nucleophile attacks preferentially at the allylic carbon atom with the largest Pd−C distance. This observation is supported by theoretical studies.[8a,9d]

Recently, we have reported on the effect of the bite angle of bidentate phosphine ligands on the structure of cationic (crotyl)-Pd(ligand) complexes and their performance in the regioselective allylic alkylation.[10] The complexes were isolated as equilibrium mixtures of two isomers, a syn and an anti isomer. Molecular modeling showed an increased embracing of the allyl moiety by the phenyl rings of the ligand when the bite angle is larger. Thus, it was predicted that an increase of the bite angle of the ligand resulted in an increase of the *cone angle* and consequently in a decrease of the syn/anti isomer ratio. Furthermore, the stoichiometric alkylation of these complexes with sodium diethyl 2-methylmalonate showed an increased regioselectivity for the branched product when the bite angle of the ligand is larger.

Scheme 3. Structures of the Complexes, Numbering Scheme, and the Ligands Used

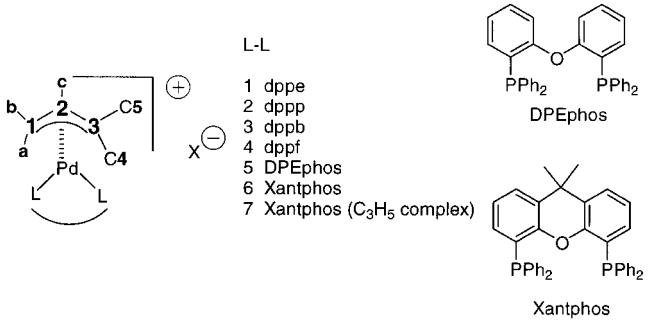

To gain more insight into the factors influencing the regioselectivity, the effect of the bite angle on the symmetry of the Pd−allyl bond was studied.

To this end, cationic (1,1-$(CH_3)_2C_3H_3$)Pd(ligand) complexes have been prepared, using ligands enforcing different bite angles (see Scheme 3). The geometry of the complexes bearing the ligands dppe (1,2-bis(diphenylphosphino)ethane), dppf (1,1′-bis(diphenylphosphino)ferrocene), DPEphos (2,2′-bis(diphenylphosphino)diphenyl ether), and Xantphos (4,5-bis(diphenylphosphino)-9,9-dimethylxanthene) was studied in detail by X-ray crystallography. The isolated complexes have been used to determine the regioselectivity in the allylic alkylation, using diethyl 2-methylmalonate as the nucleophile. In order to study the relation between the observed regioselectivity and the embracing effect of the ligand,[10] we have calculated two steric ligand parameters from the crystal structures, the cone angle[11] and the solid angle.[12]

Results

A series of cationic (ligand)Pd(1,1-$(CH_3)_2C_3H_3$) complexes (see Scheme 3) has been prepared following a standard procedure.[10] The ligand was added to the [(1,1-$(CH_3)_2C_3H_3$)-$PdCl]_2$ dimer,[13] after which the chloride anion is abstracted using either $AgBF_4$ or AgOTf. The cationic (Xantphos)Pd(C_3H_5) complex (**7**) has been prepared in a similar way, starting from the $[(C_3H_5)PdCl]_2$ dimer.

Allylic Alkylation. The complexes **1**−**6** were used in the allylic alkylation using diethyl 2-methylmalonate as the nucleophile. Upon nucleophilic attack of the malonate nucleophile two regioisomeric products can be obtained (see Scheme 4). Bond formation at C1 yields the linear product, while bond formation at C3 yields the branched product. The results of the stoichiometric reaction, presented in Table 1, show that the regioselectivity toward formation of the branched product

(8) (a) Blochl, P. E.; Togni, A. *Organometallics* **1996**, *15*, 4125−4132. (b) van Haaren, R. J.; Druijven, C. J. M.; van Strijdonck, G. P. F.; Oevering, H.; Reek, J. N. H.; Kamer, P. C. J.; van Leeuwen, P. W. N. M. *J. Chem. Soc., Dalton Trans.* **2000**, *10*, 1549−1554. (c) Ward, T. R. *Organometallics* **1996**, *15*, 2836−2838.

(9) (a) Åkermark, B.; Zetterberg, K.; Hansson, S.; Krakenberger, B.; Vitagliano, A. *J. Organomet. Chem* **1987**, *335*, 133−142. (b) Moreno-Manas, M.; Pajuelo, F.; Parella, T.; Pleixats, R. *Organometallics* **1997**, *16*, 205−209. (c) Oslob, J. D.; Åkermark, B.; Helquist, P.; Norrby, P.-O. *Organometallics* **1997**, *16*, 3015−3021. (d) Blanchadell, V.; Moreno-Manas, M.; Pajuelo, F.; Pleixats, R. *Organometallics* **1999**, *18*, 4934−4941.

(10) Van Haaren, R. J.; Oevering, H.; Coussens, B. B.; Van Strijdonck, G. P. F.; Reek, J. N. H.; Kamer, P. C. J.; Van Leeuwen, P. W. N. M. *Eur. J. Inorg. Chem.* **1999**, 1237−1241.

(11) Tolman, C. A. *Chem. Rev.* **1977**, *77*, 313.

(12) (a) White, D.; Tavener, B. C.; Leach, P. G. L.; Coville, N. J. *J. Organomet. Chem.* **1994**, *478*, 205−211. (b) Xing-Fu, L.; Xi-Zhang, F.; Ying-Ting, X.; Hai-Tung, W.; Jie, S.; Li, L. *Inorg. Chim. Acta* **1986**, *116*, 85−93. (c) White, D.; Coville, N. J. *Adv. Organomet. Chem.* **1994**, *36*, 95−158.

(13) Dent, W. D.; Long, R.; Wilkinson, A. J. *J. Chem. Soc.* **1964**, 1585−1588.

Scheme 4. Alkylation Products of Complexes **1**−**6**, X = BF_4, OTf, OAc

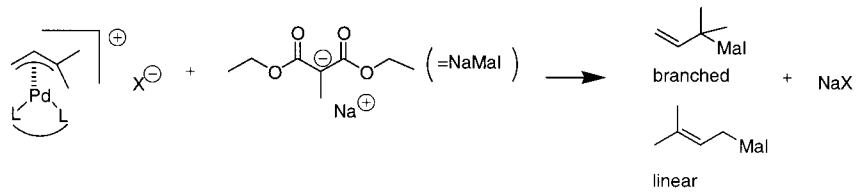

Table 1. Product Distribution in the Stoichiometric Alkylation of Complexes **1**−**6**[a]

complex	bite angle (deg)	% branched	% linear
dppe (**1**)	85.77(6)[b]	8	92
dppp (**2**)	95[c]	5	95
dppb (**3**)	99[c]	11	89
dppf (**4**)	101.2(3)[b]	13	87
DPEphos (**5**)	103.93(6)[b]	41	59
Xantphos (**6**)	108.11(7)[b]	61	39

[a] Reaction conditions are described in the Experimental Section. All experiments were carried out in triplicate; standard deviation of the reported regioselectivities is 0.5% or less. [b] Value taken from crystal structure. [c] Value taken from ref 10.

Table 2. Results of the Catalytic Alkylation of 3-Methylbut-2-enyl Acetate[a]

complex	bite angle (deg)[d]	TOF (mol/mol/h)[b]	% branched[c]	% linear[c]
dppe (**1**)	85.77(6)	400	6	94
dppf (**4**)	101.2(3)	12000	13	87
DPEphos (**5**)	103.93(6)	6200	45	55
Xantphos (**6**)	108.11(7)	2500	63	37

[a] Reaction conditions are described in the Experimental Section. All experiments were carried out in triplicate; the standard deviation of the reported regioselectivities is 0.5% or less, and the standard deviation of the reported rates is 5% or less. [b] Initial turnover frequency, determined after 2 min. [c] Determined after complete conversion. [d] Value taken from crystal structure.

increases when the bite angle of the ligand is larger, ranging from 8% for dppe (**1**) to 61% for Xantphos (**6**). In our previous work, a discrepancy was observed between the results of stoichiometric and catalytic alkylation due to competition between syn−anti isomerization and alkylation.[8b,10] In this investigation, we found that in the absence of syn and anti isomeric complexes, the stoichiometric and the catalytic reaction show similar regioselectivities (Table 2). The rate of the catalytic reaction is dependent on the ligand, being relatively slow for dppe (**1**) and relatively fast for dppf (**4**).

NMR Experiments. The effect of the ligand on the allyl moiety is reflected in the NMR spectra of the complexes. In the ^{1}H NMR of complexes **1**−**6**, the signals of the two methyl groups of the allyl moiety appear as separate signals. The chemical shift is dependent on the ligand and is found at higher field when the bite angle of the ligand is larger (Table 3).

At room temperature, the signals of Ha and Hb are broadened in all cases, especially for complexes bearing ligands with a large bite angle. The signal of Hc appears as a triplet due to coupling with the Ha and Hb nuclei. The phosphorus spectra show two different signals, which are broad for the Xantphos-modified complex (Table 3).

The broadened signals indicate the occurrence of dynamic exchange of the allyl moiety,[16] which appears to proceed at a higher rate when the bite angle of the ligand is larger. Therefore, a NOESY spectrum was recorded for complex **6** bearing the Xantphos ligand, which enforces a large bite angle. The methyl groups appeared to have a steric interaction with the phenyl rings of the ligand. This interaction was studied in more detail by recording NOE difference spectra, in which the methyl groups were irradiated. Irradiation of the signal at 0.92 ppm, which was assigned to the *syn*-CH_3 on the basis of the value of ^4J(P−CH_3), showed that this CH_3 group has a strong interaction with Hc. In contrast, the irradiation of the CH_3 signal at 1.04 ppm shows a much weaker interaction. These observations confirm the assignment of the signals to respectively the *syn*- and *anti*-CH_3 groups. The two CH_3 groups differ in interaction with the phenyl groups of the ligand. The interaction is stronger for the *syn*-methyl than for the *anti*-methyl group. This results in a shielding effect of the *syn*-CH_3 group in complex **6**, which is reflected in its resonance at unusually high field.

Table 3. Selected NMR Data of the Complexes **1**−**7**, Data Determined at 298 K

complex (ligand)	bite angle (deg)	line width ^{31}P (Hz)	δ Me syn	δ Me anti
1 (dppe)	85.77(6)[a]	8	1.90	1.45
2 (dppp)	95[b]	9	1.28	1.13
3 (dppb)	99[b]	6	1.36	0.82
4 (dppf)	101.2(3)[a]	3	1.11	1.11
5 (DPEphos)	103.93(6)[a]	10	1.23	1.06
6 (Xantphos)	108.11(7)[a]	91	0.92	1.04
7 (Xantphos)	108.11(7)[a]	3		

[a] Value taken from crystal structure. [b] Value taken from ref 10.

The dynamic exchange of the allyl moiety of complex **6** has been studied in detail by means of variable-temperature NMR. At −40 °C the slow exchange limit is reached. Upon raising the temperature, apart from Ha and Hb, also the two methyl groups of the ligand backbone, which appear as separate signals due to its folded structure (see below), and the two phosphorus atoms exhibit exchange. Rate data obtained from simulation of the spectra show that the observed dynamic behavior is the result of two different processes. The exchange of the methyl groups of the ligand and the phosphorus atoms occurs with the same rate (k = 450 s^{-1} at 303 K, $\Delta H^{\ddagger}_{298}$ = +71 kJ/mol, $\Delta S^{\ddagger}_{298}$ = −88 J/mol K), which is significantly higher than that of the Ha−Hb exchange (k = 100 s^{-1} at 303 K, $\Delta H^{\ddagger}_{298}$ = +56 kJ/mol, $\Delta S^{\ddagger}_{298}$ = −30 J/mol K).

X-ray Structures. The influence of the bite angle on the steric interaction of the ligand with the allyl moiety was also studied by X-ray crystallography. After recrystallization from CH_2Cl_2/hexane we have obtained crystals suitable for X-ray structure determination of the cationic (ligand)palladium(1,1-$(CH_3)_2C_3H_5$) complexes with the ligands dppe (**1**), dppf (**4**) and DPEphos (**5**), whereas no suitable crystals were obtained of complexes

(14) Kranenburg, M.; Delis, J. P. G.; Kamer, P. C. J.; van Leeuwen, P. W. N. M.; Veldman, N.; Spek, A. L.; Goubitz, K.; Fraanje, J. *J. Chem. Soc., Dalton Trans.* **1997**, 1839−1849.
(15) Guari, Y.; van Strijdonck, G. P. F.; van Leeuwen, P. W. N. M.; et al. Submitted for publication.
(16) (a) Vrieze, K.; van Leeuwen, P. W. N. M. *Dynamic Nuclear Magnetic Resonance Spectroscopy*; Academic Press: New York, 1975. (b) Hansson, S.; Norrby, P.-O.; Sjögren, M. P. T.; Åkermark, B.; Cucciolito, M. E.; Giordano, F.; Vitagliano, A. *Organometallics* **1993**, *12*, 4940−4948.

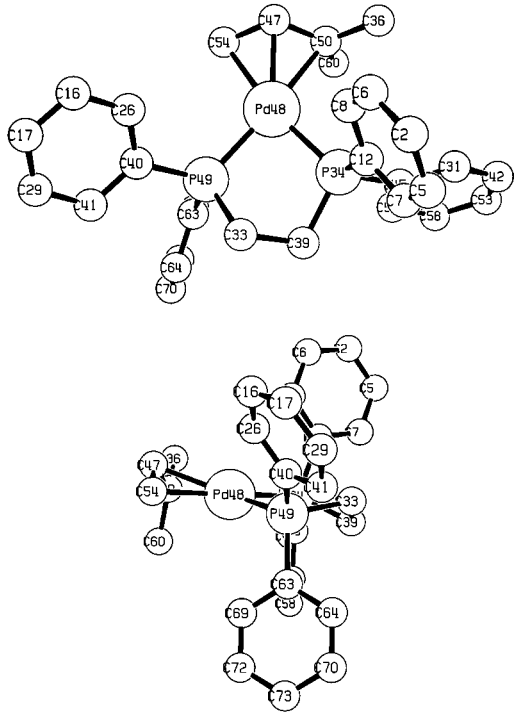

Figure 1. Two views of the crystal structure of complex **1** (dppe).

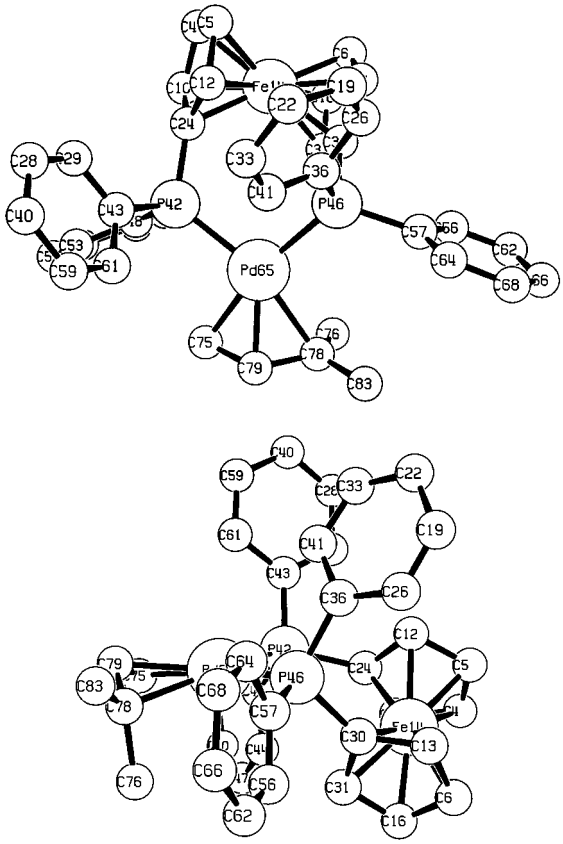

Figure 2. Two views of the crystal structure of complex **4** (dppf).

bearing ligands with a bite angle larger than DPEphos. To study the coordination mode of the Xantphos ligand, the cationic (Xantphos)Pd(C_3H_5) complex has been prepared and crystallized.

Selected structural data obtained from the X-ray structures (Figures 5−8) are presented in Tables 4 and 5.

All structures are cationic, since the counterion is located at a large, nonbonding distance from palladium. In all complexes

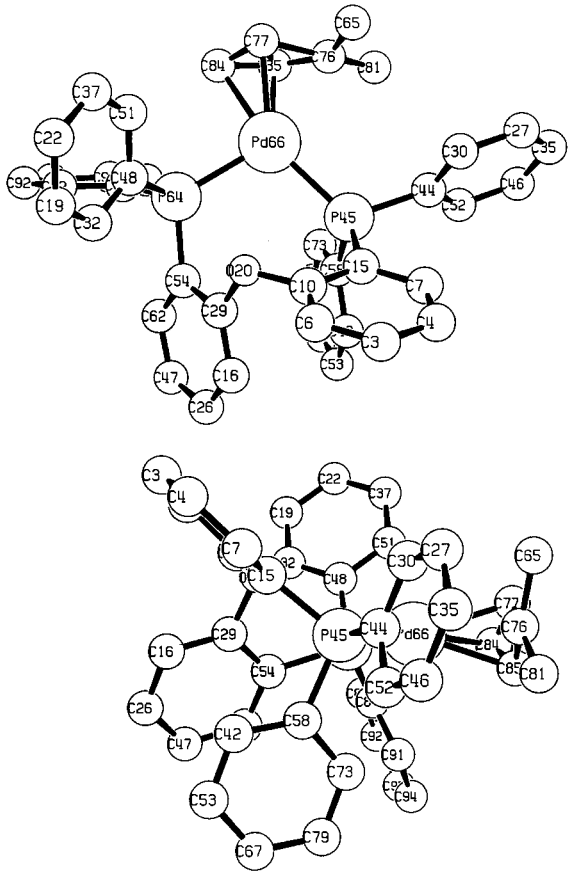

Figure 3. Two views of the crystal structure of complex **5** (DPEphos).

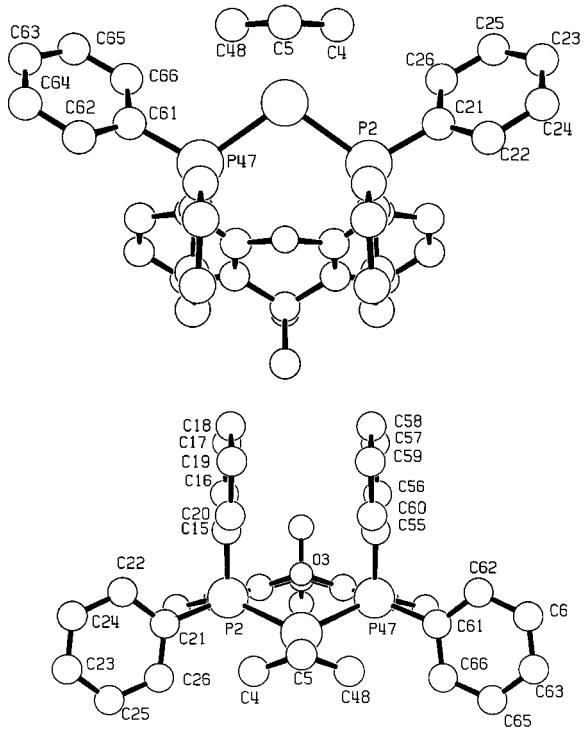

Figure 4. Two views of the crystal structure of complex **7** (Xantphos).

two phenyl rings of the ligand, located in the P−Pd−P plane, point in the direction of the allyl moiety. The planes of the -$C(CH_3)_2$ fragment and the closest phenyl ring are almost parallel (Table 5). The two other phenyl ring of the ligand point in the same direction as C2.

The DPEphos ligand (β = 103.93(6)°) shows an interaction

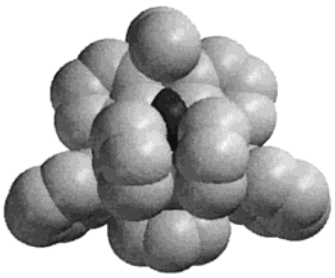

Figure 5. Space-filling model of the X-ray structure of complex **7**.

Table 4. Selected Bond Distances (Å) Obtained from the Crystal Structures

parameter	**1** (dppe)	**4** (dppf)	**5** (DPEphos)[a]	**7** (Xantphos)
Pd−C1	2.185(9)	2.192(15)	2.161(7)	2.17(1)
Pd−C2/C2a	2.174(7)	2.152(16)	2.21(1)	2.16(1)
Pd−C2b			2.21(1)	
Pd−C3	2.253(7)	2.291(18)	2.37(1)	2.17(1)
C1−C2	1.42(1)	1.42(2)	1.39(1)	1.34(2)
C1−C2			1.28(1)	
C2/C2a−C3	1.41(1)	1.41(2)	1.41(2)	1.34(2)
C2b−C3			1.59(2)	
C3−C4 (anti)	1.51(1)	1.58(2)	1.48(1)	
C3−C5 (syn)	1.50(1)	1.44(2)	1.48(1)	
Pd−P (cis to C1)	2.296(2)	2.313(6)	2.336(2)	2.372(2)
Pd−P (cis to C3)	2.293(2)	2.33(9)	2.379(2)	2.372(2)

[a] C2a corresponds to C85 in Figure 3, and C2b corresponds to C77 in Figure 3.

between one of the aromatic rings (C- -C) of the backbone and one of the phenyl rings bound to phosphorus (C- - -C) (Figure 3). The angle between the two planes is 23.8(2)°, and the minimum distance is 3.37(3) Å (*d*(C54−C58)). This type of orientation for DPEphos has also been observed in the two other crystal structures known of palladium complexes of this ligand, the zerovalent (tcne)Pd(DPEphos) complex[14] and the (DPEphos)Pd(*p*-C_6H_4CN)Br complex.[15]

With respect to C2, the ferrocene unit of the dppf ligand is located under the P−Pd−P plane and is twisted as a result of its staggered conformation (Figure 2). The two Cp rings are staggered and almost parallel (angle = 3.6(5)°). Also in this complex, two phenyl rings of the ligand point in the direction of the allyl moiety.

The Xantphos complex (Figure 4) has C_s symmetry, two phenyl rings of the ligand point in the direction of the allyl moiety, and two are directed upward with respect to C2. The latter phenyl groups are almost parallel (13.4(2)°), and the distance between the ipso carbon atoms is 3.87(2) Å.

The two aromatic rings in the backbone of the Xantphos ligand are not coplanar as a result of the sp_3 carbon atom and the oxygen atom in the bridge. The value found for the angle between the planes (27.4(5)°) is similar to that found for the zerovalent (tcne)Pd(Xantphos) complex reported previously.[14] As a result of this folded structure, one of the methyl groups of the backbone is located equatorially and one axially, resulting in two different signals in the NMR spectrum (see above).

As expected, the C1−C2−C3 plane is not perpendicular to the P−Pd−P plane. The angle between these planes appears to be dependent on the ligand, as it ranges from 114.4(9)° for dppe to 100(2)° for Xantphos (Table 5). In all C_5H_9 complexes, the allyl moiety is not symmetrically bound to the palladium center. The Pd−C1 bond is shorter than the Pd−C3 bond, and the C1−C2 bond is longer than the C2−C3 bond (Table 4). Considering these differences between the bond lengths, the nonsymmetry of the allyl moiety is more pronounced when the bite angle of the ligand is larger.

In the complex of dppe, the bond between C3 and the *syn*-methyl substituent on the allyl moiety is slightly shorter (1.50(1) Å) than the bond from C3 to the anti substituent (1.51(1) Å). When the bite angle is larger, as in the case of dppf, the C3−C5(syn) bond becomes shorter (1.44(2) Å) and the C3−C4(anti) bond is longer (1.58(2) Å).

It has been reported that in some cases the allyl moiety is slightly rotated around the Pd−allyl axis.[4c,d,9] This rotation toward a product-like state could be important for determining the regioselectivity. In the crystal structures we present here, no significant rotated orientation of the allyl group is observed and no correlation with the bite angle of the ligand is found (Table 5).

The palladium phosphorus distances are in same range as found previously for zerovalent (P-P)Pd(tcne) complexes.[14] In general, the bond between palladium and phosphorus cis to C1 is shorter than that to phosphorus cis to C3. This difference is more pronounced when the bite angle of the ligand is larger; it is approximately zero for the dppe-ligated complex and amounts to 0.02 Å for dppf (**4**) and to 0.04 Å for DPEphos (**5**). The distance between palladium and the phosphorus atoms is also dependent on the bite angle of the ligand. A smaller bite angle results in a smaller Pd−P distance. It ranges from 2.293(2) Å for dppe to 2.372(2) Å for Xantphos.

Cone Angle, Solid Angle. From the above observations it is clear that the bite angle of the ligand influences the symmetry of the Pd−allyl bond via steric interaction. The top views of the crystal structures show that the phenyl rings are closer to the allyl moiety when the bite angle of the ligand is larger, as was already suggested in a previously reported molecular modeling study.[10] The bite angle, however, is an indirect parameter for determining the amount of steric interaction a ligand induces. Therefore we decided to determine the values of two direct parameters from the X-ray structures, the cone angle θ,[11] introduced by Tolman, and the solid angle Ω,[12] as introduced by Bagnall and Xing-Fu.

The results in Table 6 show in general the same trend for each of these geometrical parameters. Going from dppe to Xantphos, the bite angle, the cone angle, and the solid angle increase.

Discussion

Structure of the Complexes in the Solid State. From the X-ray data, it can be concluded that the presence of substituents on the allyl moiety distorts the symmetry of the bond to palladium (see Scheme 5). This effect has been observed before, both in other crystal structures and in modeling studies.[4c−e,9] In all cases, it is observed that the bonding distance between C3 and palladium is longer than between palladium and C1. The weakened bonding between the substituted allylic site and palladium corresponds to an enhanced bond strength of the allylic C2−C3 bond. In the present case, the distortion is dependent on the ligand used and, specifically, on the bite angle of the ligand used. A larger bite angle results in an increase of the cone angle of the ligand and therefore in a more pronounced embracing of the allyl moiety by the phenyl rings of the ligand (see Table 6). The increase in solid angle with larger bite angle indicates that there is less space for the allyl ligand to coordinate to palladium. In Figure 5, a space-filling model of the crystal structure containing the Xantphos ligand is presented. There is enough space for the allyl moiety to coordinate, but addition of two extra methyl substituents on one of its terminal positions will result in significant steric interaction (see Figure 5). This leads to a lengthening of the Pd−C3 bond and changes in bond

Table 5. Selected Geometrical Data Obtained from the Crystal Structures

parameter	**1** (dppe)	**4** (dppf)	**5** (DPEphos)	**7** (Xantphos)
∠(P−Pd−P) (deg)	85.77(6)	101.2(3)	103.93(6)	108.11(7)
∠(C−C−C) (deg)	121.2(7)	124(1)	120.2(7), 115(1)[a]	120(2)
d(C5(syn)−(closest Ph plane)) (Å)	3.44(2)	3.54(3)	3.20(1)[b]	
d(C1−(PPdP plane)) (Å)	+0.044(10)	−0.17(2)	+0.319(8)	−0.35(1)
d(C2−(PPdP plane)) (Å)	−0.440(10)	−0.35(3)	+0.91(1)[a] −0.47(1)[a]	−1.01(2)
d(C3−(PPdP plane)) (Å)	+0.329(9)	+0.34(3)	−0.13(1)	−0.348(3)
∠((CCC plane)−(PPdP plane)) (deg)	114.4(9)	114(2)	111(1)[a] 99(1)[a]	100(2)
∠((C4−C3−C5 plane)−(closest Ph plane)) (deg)	7.9(5)	5(1)	10.2(7)	

[a] C2a corresponds to C85 in Figure 3 and C2b corresponds to C77 in Figure 3. [b] C81 in Figure 3.

Table 6. Values of the Bite Angle, the Cone Angle, and the Solid Angle, as Determined from the X-ray Structures

complex	bite angle (deg)	cone angle (deg)	solid angle (sr)	% branched product
1 (dppe)	85.77(6)	224.6	4.47	8
4 (dppf)	101.2(3)	229.7	5.44	11
5 (DPEphos)	103.93(6)	240.2	5.00	41
7 (Xantphos)	108.11(7)	246.9	5.56	61

Scheme 5. Schematic Representation of the Distortion of the Pd−Allyl Bond as Observed in the X-ray Structures

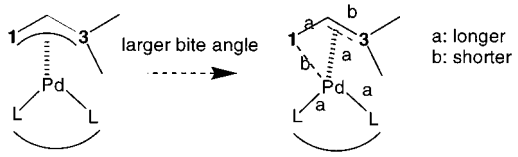

lengths as shown in Scheme 5. Therefore it is argued that the steric effect of the bite angle on the dissymmetry of the Pd−allyl bond induces electronic effects on the allyl moiety.

The distortion of an η^3 toward an η^1,η^2 bonding mode as observed in the crystal structures will result in a lower value of the overlap integral on the η^2 site and a higher value of this integral on the η^1 site. On the η^2 site, both the donating interaction (ligand to metal) and the back-donating interaction (metal to ligand) will be decreased with respect to the symmetrically π-bonded allyl moiety.[8c,9] Thus, as a result of the lengthening of the Pd−C3 distance the back-donation to the LUMO of this site of the allyl moiety is lower than in a symmetically bonded π-allyl moiety. At the same time, the Pd−C1 distance is decreased and the C1−C2 distance is increased, which both indicate an increase in the L→M donation as well as the M→L back-donation on the η^1 site of the allyl moiety.

The difference in the two allylic binding sites is reflected in the bond between palladium and phosphorus. The Pd−P cis to the nonsubstituted C1 is shorter than the bond trans to C1. So, the two ligands that are most strongly bound to the metal center are cis to one another.

The effects of changes in donation and back-donation are also reflected in the value for the angle between the allylic CCC plane and the P−Pd−P plane. In the absence of back-donation, a value close to 90° would be expected. When the back-donation to C1 and C3 is strong, the value for this angle (∠((CCC)−(PPdP))) will increase. In the crystal structures presented in this paper, the value of ∠((CCC)−(PPdP)) is dependent on the ligand. When the bite angle of the ligand is larger, this angle decreases. It is concluded that an increase in the bite angle results in a decrease of the back-donation. As a consequence, the allylic LUMO orbitals, which are the sites of reaction in the nucleophilic attack, remain less occupied. Therefore, a larger bite angle of the ligand results in an increase of the reactivity of the allyl moiety toward nucleophilic attack. This has indeed been observed in the catalytic alkylation of *trans*-but-2-enyl acetate.[10]

Structure of the Complexes in Solution. The NOE experiments carried out on the cationic (1,1-$(CH_3)_2C_3H_3$)Pd(Xantphos)$^+$ complex (**6**) revealed steric interactions between the methyl groups and the phenyl rings of the ligand. The phenyl rings show the strongest interaction with the *syn*-methyl, compared to the *anti*-methyl group, whereas in the X-ray structure of complex **7**, the anti hydrogen atom is closest to the phenyl rings. A slight rotation about the P−C bond in the X-ray structure would bring the phenyl rings at a closer distance to the syn substituent than to the anti substituent. In solution, some rotation about the P−C bond may take place, and our results indicate that on average the syn substituent is at a closer distance to the phenyl rings. The crystal structures show that the steric interaction is stronger when the bite angle of the ligand is larger.

Complex **6**, as well as the other complexes, can in theory be present in two pairs of enantiomeric structures (Scheme 6): the methyl groups can be oriented trans to P1 or trans to P2, and the axial phenyl rings of the ligand (Figures 1−4) can be oriented in the same direction as C2 (endo) or in the opposite direction (exo). In the crystal structures, only the endo isomer is found for complexes **1**, **4**, and **7**, whereas for complex **5** both isomers are found to crystallize together. In the NMR spectra only one complex is observed, also at low temperature, which is therefore assigned to be the endo isomer. It cannot be ruled out that the different complexes which are present at reaction temperature show different regioselectivities in the allylic alkylation.

Variable-temperature NMR experiments carried out for complex **6** showed that several types of fluxional behavior occur at the same time. The slower process involves the Ha/Hb exchange, and the faster process involves the phosphorus atoms and the two methyl groups of the ligand, which at low temperature appear as separate signals due to the folded structure of the backbone (see above). The exchange of the methyl groups of the ligand indicates that, during the faster process, the backbone of the ligand folds from one orientation to the other, thereby exchanging the methyl groups from an equatorial to an axial position and vice versa.

The relatively high negative value for the entropy of activation suggests that the faster process occurs via an associative pathway. It is known that temporary coordination of the counterion of cationic (allyl)palladium complexes may enhance the rate of dynamic exchange of the allyl moiety.[16b] In a thus formed five-coordinated Pd(allyl) complex, the so-called apparent rotation of the allyl moiety can easily take place.[16b] In complex **6**, such a process will cause the exchange of C1 and C3 and vice versa, resulting in the equivalency of the two phosphorus atoms. Apparently, during this process, the backbone

Scheme 6. Two Pairs of Enantiomers of Complex **6**

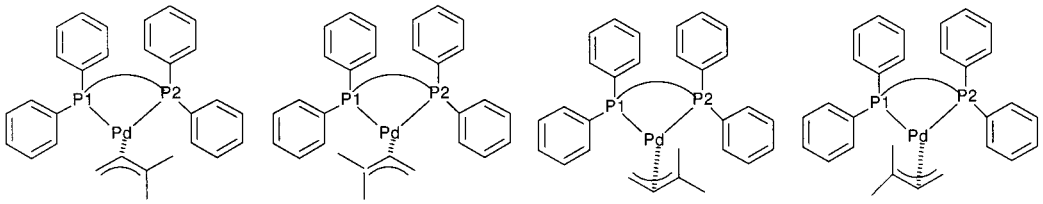

Scheme 7. Different Intermediates for the $\pi-\sigma$ Rearrangement

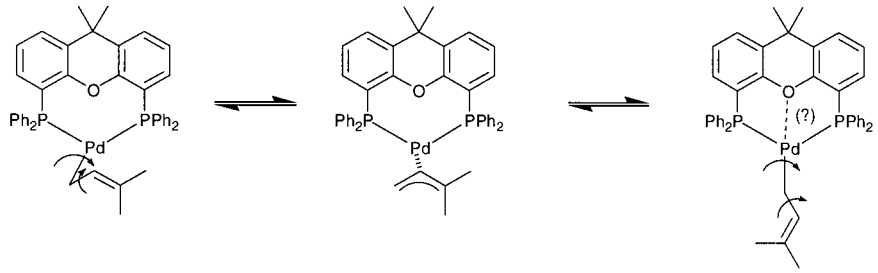

of the ligand changes its folded structure from one form to the other, thereby exchanging the two methyl groups of the ligand.

The Ha/Hb exchange, observed in the slower process, is known to be caused by a $\pi-\pi$ rearrangement.[17] The Pd−C3 and Pd−C2 bonds are broken selectively, and a Pd−C1 σ-bond is formed. Rotation about the Pd−C1 bond and the C1−C2 bond results in an exchange of the signals of Ha and Hb. As at −40 °C only one complex is observed, it is concluded that, contrary to our previous results,[8b] the $\pi-\sigma$ rearrangement of the allyl moiety observed for complex **6** does not lead to the exchange of the endo and exo isomeric forms of the complex.

If the $\pi-\sigma$ rearrangement process occurs via a T-shaped palladium intermediate, in which no exchange of the coordination sites of C1 and C3 takes place, the exchange of endo to exo and vice versa will take place.[8b] On the other hand, if it occurs via a C_s-symmetric Y-shaped intermediate, in which a C1−C3 exchange will take place, the endo−exo exchange may not occur (Scheme 7). Recently, we have found evidence for coordination of the oxygen atom of the ligand backbone to palladium in cationic (Xantphos)Pd(Ph) complexes.[15] This may also occur in the Y-shaped intermediate. The thus formed flat structure of the backbone can fold back to form the endo isomer of the $\pi-\sigma$ rearranged complex. Because the $\pi-\sigma$ rearrangement is the slower process, it cannot be distinguished whether it involves a T- or a Y-shaped intermediate.

Allylic Alkylation. Several theoretical studies concerning the mechanism of the allylic alkylation reaction have been reported in the literature.[9d,17] Recently, a theoretical rationale has been presented[9d] for the correlation between the regioselectivity and the nonsymmetry of the allyl moiety.[9] By means of DFT calculations (ADF), it was shown that an electronic preference for initial nucleophilic attack on the carbon atom of the allyl moiety with the largest Pd−C distance leads to a lowering of the energy barrier encountered in a later stage of the reaction. Our results may be explained following the same rationale.

First, the malonate nucleophile selects the site of attack, based on electronic properties (charge, LUMO coefficients) and steric (accessibility) properties. Therefore, the regioselectivity for initial attack at C3 will be a tradeoff between the larger steric hindrance the nucleophile encounters during attack at this position and the electronic preference.

During the process of bond formation,[17] the allyl moiety rotates to form a transient palladium−olefin complex.[18] When the attack takes place at C3, the branched site, a terminal C=C double bond is formed. The formation of the transient palladium−olefin complex implies that the substituted carbon atom has been rotated out of the P−Pd−P plane, thereby minimizing the steric interaction with the phenyl rings of the ligand.

Alternatively, attack on C1 results in the formation of an internal C=C double bond, substituted by three groups. In the resulting palladium−olefin complex, the methyl substituents are at a closer distance to palladium than they were in the allyl complex, so the steric hindrance with the ligand is increased. In this stage of the reaction, the height of the energy barrier is also influenced by the thermodynamically favorable formation of an internal C=C double bond compared with that of a terminal alkene.

The preference for formation of the branched product when the bite angle of the ligand is larger can therefore be explained in both steric and electronic terms. Thus, the selectivity toward the formation of the linear product for the dppe-ligated complex can be explained by a less activated allyl moiety due to less steric interaction with the ligand (see above). Consequently, the steric accessibility of C3 relative to C1 is important. Also in the second stage of the reaction, when the more favored internal alkene is formed, the steric hindrance in the palladium−olefin complex will be less than that in complexes of the other ligands.

In contrast, the use of ligands with a larger bite angle will result in the formation of a more activated allyl moiety in the corresponding palladium complex. In the tradeoff between steric access and electronic reactivity, the electronic factors may prevail. During the rotation of the allyl moiety, the steric hindrance encountered during terminal olefin formation (branched product) will be less than that for internal olefin formation (linear product). We therefore propose that the regioselectivity of the

(17) (a) Hagelin, H.; Åkermark, B.; Norrby, P.-O. *Chem.—Eur. J.* **1999**, *5*, 902−909. (b) Suzuki, T.; Fujimoto, H. *Inorg. Chem.* **1999**, *38*, 370−382. (c) Hagelin, H.; Svensson, M.; Åkermark, B.; Norrby, P.-O. *Organometallics* **1999**, *18*, 4574−4583.

(18) Steinhagen, H.; Reggelin, M.; Helmchen, G. *Angew. Chem., Int. Ed. Engl.* **1997**, *36*, 2108−2110.

Scheme 8 Tradeoff Pathways That May Determine the Regioselectivity

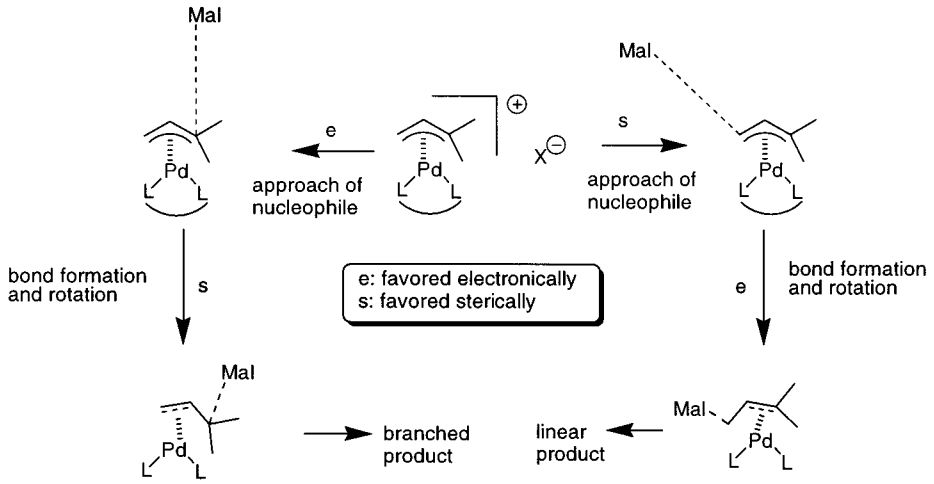

allylic alkylation is determined by a set of steric/electronic tradeoff pathways (see Scheme 8).

The large difference in the amount of branched product formed from the dppf (**4**) and the DPEphos (**5**) modified complexes would not be expected on the basis of the small difference in bite angle. In general, comparing the values found for the three different ligand parameters (bite angle, cone angle, solid angle) with the regioselectivity, reveals that the cone angle shows the best correlation.

The total effect of the ligand geometry on the rate of the *catalytic* reaction is dependent on several effects. The reaction consists of a number of consecutive stages: (1) substrate coordination to palladium, (2) oxidative addition, (3) nucleophilic attack, and (4) product dissociation. A large cone angle will slow down stage 1, as a result of large steric hindrance. The study of the crystal structures shows that a large cone angle may enhance the reaction rate of stages 3 and 4. The oxidative addition process can be regarded as the reverse process of nucleophilic attack, so it can be expected that also stage 2 may proceed faster when the cone angle is larger. Thus, the total effect of the cone angle of the ligand on the rate is determined by a tradeoff between the accelerating and the decelerating effects.

Conclusion

We have shown that in crystal structures an increase of the bite angle of a bidentate phosphorus ligand leads to an increase in both the cone angle and solid angle of the ligand. As the effect of the ligand on the geomety and reactivity of the complexes is best described in terms of steric hindrance, the cone angle of the ligand is the parameter of choice.

The more pronounced embracing of the allyl moiety by the ligand distorts the symmetry of the Pd−(1,1-$(CH_3)_2C_3H_3$) bond to an η^1,η^2-type coordination. Furthermore, the back-bonding to the substituted site of the allyl moiety decreases when the cone angle is large. This sterically induced electronic effect has a pronounced influence on the reactivity of the allylic carbon atoms and the regioselectivity of stoichiometric alkylation.

A larger cone angle of the ligand enhances the electronic preference for nucleophilic attack on the branched position, but also the steric hindrance at this position is enhanced. Therefore it is concluded that the regioselectivity of the reaction is a result of a tradeoff between electronic and steric interactions.

Experimental Section

^{1}H (300 MHz, TMS, $CDCl_3$) and $^{31}P\{^1H\}$ (121.5 MHz external 85% H_3PO_4, $CDCl_3$) NMR spectra were recorded on a Bruker AMX-300 spectrometer.

The product distribution of allylic alkylation was measured on an Interscience Mega2 apparatus, equipped with a DB1 column, length 30 m, inner diameter 0.32 mm, film thickness 3.0 μm, and a FID detector.

All experiments were carried out using standard Schlenk techniques. All solvents were freshly distilled prior to use. All reactions have been performed at room temperature (292 K).

The variable-temperature NMR experiments have been carried out by measuring spectra at different temperatures, ranging from 233 K (dynamic behavior frozen out) to 328 K (coalesced signals, toward fast exchange). The simulation of the spectra was carried out using gNMR software.[19]

Sodium diethyl 2-methylmalonate (0,5 M in THF) was prepared from diethyl 2-methylmalonate and NaH in THF at 273 K. All alkylation experiments were carried out in triplicate.

The stoichiometric alkylation reactions were performed by adding an excess of sodium diethyl 2-methylmalonate (0.1 mL of a 0.5 M solution in THF) to a solution of 10 mg of the Pd complex in 1 mL of THF. Reaction was instantaneous, and after 1 min, the mixture was worked up with water, filtered over silica, and analyzed by GC.

The catalytic reactions were performed in THF (10 mL), using 0.05 mol % of catalyst (0.00050 mmol), 1.0 mmol of 3-Me-but-2-enyl acetate, and 2.0 mmol of sodium diethyl 2-methylmalonate. The reaction was monitored by taking samples from the reaction mixture, which, after quenching with wet ether, were analyzed by GC using decane as the internal standard.

The Pd complexes were prepared in CH_2Cl_2 from $[(C_5H_9)Pd\text{-}\mu\text{-}Cl]_2$[13] by adding 2 equiv of ligand and abstracting the Cl atom with AgOTf.[10] The complexes were isolated in quantitative yield (white microcrystalline powder) as their analytically pure equilibrium mixtures and were used as such in the alkylation reaction. The syntheses of DPEphos and Xantphos have been published elsewhere.[6] Dppe, dppp, dppb, and dppf were obtained from Acros chemicals and used as received.

(C_5H_9)Pd(dppe)OTf (1). ^{1}H: 1.05 (t, 3H, $J_1 = J_2 = 6.3$ Hz, *anti*-CH_3); 1.90 (t, 3H, $J_1 = J_2 = 8.4$ Hz, *syn*-CH_3); 2.5−2.8 (br m, 4H, 2P−CH_2); 3.6−4.0 (br, 2H, allylic-CH_2); 5.53 (t, 1H, $J_1 = J_2 = 11.0$ Hz); 7.3−7.9 (br m, 20H, aromatic H).

^{31}P: 46.8 (d, 1P, $J = 34$ Hz); 51.1 (d, 1P, $J = 34$ Hz).

$^{13}C\{^1H\}$: 20.2 (d, $J = 5$ Hz); 26.6 (d, $J = 13.7$ Hz); 26.8; 26.9 (d, $J = 13$ Hz); 28.0 (d, $J = 13$ Hz); 28.5 (d, $J = 13$ Hz); 60.6; 61.0; 103.5; 104; 107.9; 108.2; 115.0; 115.1; 115.2; 116.7; 116.8; 117.1; 117.3; 129.5 (d, $J = 11$ Hz); 131.8;132.3 (d, $J = 13$ Hz).

(19) Budzelaar, P. H. M. gNMR version 3.5 M, Ivorysoft, Amerbos, Amsterdam, 1995.

Table 7. Crystallographic Data for Compounds **1**, **4**, **5**, and **7**

	1	**4**	**5**	**7**
formula	$[C_{31}H_{33}OP_2Pd]^+ SO_3CF_3^-$	$[C_{39}H_{37}P_2FePd]^+ BF_4^-$	$[C_{41}H_{37}OP_2Pd]^+ BF_4^-$	$[C_{42}H_{37}OP_2Pd]^+ BF_4^- \cdot CH_2Cl_2$
λ, Å	1.5418	1.5418	1.5418	1.5418
a, Å	10.9718(9)	15.827(3)	11.822(1)	9.153(2)
b, Å	16.101(2)	13.067(2)	12.519(2)	18.0851(9)
c, Å	18.681(1)	18.267(3)	14.435(2)	12.6484(8)
α, deg			83.84(1)	
β, deg	91.601(4)	108.01(1)	78.01(1)	105.409(9)
γ, deg			67.568(8)	
V, Å^3	3298.8(5)	3592.7(11)	1930.7(5)	2018.5(5)
space group	$P2_1/c$	Cc	$P\bar{1}$	$P2_1/m$
Z	4	4	2	2
fw	723.0	816.7	800.8	812.9
ρ(obs), g cm^{-3}	1.46	1.51	1.38	1.48
μ, cm^{-1}	64.6	85.2	50.8	61.1
T, K	293	293	255	293
R^a	0.065	0.067	0.059	0.091
$R_w{}^b$	0.067	0.080	0.061	0.103

^{a} $R = \sum(||F_{obs}| - k|F_{calc}||)/\sum(|F_{obs}|)$. ^{b} $R_w = \sum w((|F_{obs}| - k|F_{calc}|)^2)/\sum(|F_{obs}|^2)$.

HR-MS (FAB): $C_{31}H_{33}P_2Pd^+$ requires 573.1092 g/mol, found 573.1102 g/mol.

(C_5H_9)Pd(dppp)OTf (2). ^{1}H: 1.14 (dd, 3H, $J_1 = J_2 = 6.3$ Hz, *anti*-CH_3); 1.28 (dd, 3H, $J_1 = J_2 = 9.6$ Hz, *syn*-CH_3); 1.6 (br m, 1H, C(H)-*H*$-CH_2-$P); 2.2 (br m, 1H, C(H)*H*$-CH_2-$P); 2.75 (m, 2H, $-CH_2-$P); 2.8 (dd, 1H, $J_1 = J_2 = 13$ Hz, allylic H); 2.95 (m, 2H, $-CH_2-$P); 3.65 (dd, 1H, $J_1 = J_2 = 7.2$ Hz, allylic H); 5.27 (dd, 1H, $J_1 = 8.1$ Hz, $J_2 = 13.8$ Hz, allylic H); 7.2−7.7 (br m, 20H, aromatic H).

^{31}P: 6.5 (d, $J = 65.7$ Hz); 9.8 (d, $J = 65.3$ Hz).

^{13}C{^{1}H}: 19.0; 20.7; 25.9; 26.3; 26.6; 64.1 (d, $J = 29$ Hz); 110.1 (d, $J = 26$ Hz); 114.5; 128.4; 129.2; 129.3; 129.5; 129.6; 130.5; 131.0; 131.8; 131.9; 132.7 (d, $J = 11$ Hz); 133.8 (d, $J = 12.4$ Hz); 134.3 (d, $J = 14$ Hz).

HR-MS (FAB): $C_{32}H_{35}P_2Pd^+$ requires 587.1249 g/mol, found 587.1255 g/mol.

(C_5H_9)Pd(dppb)BF_4 (3). ^{1}H: 0.82 (dd, 3H, $J_1 = J_2 = 6.0$ Hz, *anti*-CH_3); 1.36 (dd, 3H, $J_1 = 7.4$ Hz, $J_2 = 10.1$ Hz, *syn*-CH_3); 1.7 (br m, 4H, CH_2-CH_2-P); 2.7 (br m, 5H, CH_2-CH_2-P, allylic H); 3.7 (br, 1H, allylic H); 5.45 (t, 1H, $J_1 = J_2 = 10.8$ Hz); 7.2−7.8 (br m, 20H, aromatic H).

^{31}P: 21.3 (d, AB, 1P, 49 Hz); 22.2 (d, AB, 1P, 48 Hz).

^{13}C{^{1}H}: 20.0; 22.9; 25.4; 26.3; 26.9; 63.1; 106.1; 106.9; 113.9; 116.5; 116.6; 129.2; 130.7; 131.3; 134.2; 135.0.

HR-MS (FAB): $C_{33}H_{37}P_2Pd^+$ requires 601.1405 g/mol, found 601.1400 g/mol.

(C_5H_9)Pd(dppf)BF_4 (4). ^{1}H: 1.1 (m, 6H, $2CH_3$); 2.82 (t, 1H, $J_1 = J_2 = 11.4$ Hz, *anti*-allylic H); 3.68 (t, $J_1 = J_2 = 7.2$ Hz, *syn*-allylic H); 3.87 (s, 1H, FcH); 4.19 (s, 1H, FcH); 4.27 (s, 1H, FcH); 4.32 (s, 1H, FcH); 4.41 (s, 1H, FcH); 4.48 (s, 2H, FcH); 4.55 (s, 1H, FcH); 5.49 (dd, 1H, $J_1 = 8.1$ Hz, $J_2 = 13.8$ Hz, Hc); 7.3−7.6 (br m, 18 H, aromatic H); 7.85 (br m, 2H, aromatic H).

^{31}P: 22.7 (d, 1P, $J = 46$ Hz); 26.9 (d, 1P, 46 Hz).

^{13}C{^{1}H}: 15.5; 21.1; 26.5; 66.1; 114.3; 116.0; 118.4; 129.2; 129.3; 129.4; 129.5; 129.6; 130.3; 130.8; 131.3; 131.4; 131.5; 132.1; 132.4; 132.6; 132.6; 133.1; 133.5; 134.0; 134.4; 134.9.

HR-MS (FAB): $C_{39}H_{37}FeP_2Pd^+$ requires 729.0755 g/mol, found 729.0748 g/mol.

(C_5H_9)Pd(DPEphos)BF_4 (5). ^{1}H: 1.06 (t, 3H, $J_1 = J_2 = 5.6$ Hz, *anti*-CH_3); 1.23 (dd, 3H, $J_1 = 5$ Hz, $J_2 = 11$ Hz, *syn*-CH_3); 2.84 (t, 1H, $J_1 = J_2 = 12.5$ Hz, *anti*-allylic H); 3.63 (dt, 1H, $J_1 = J_2 = 7.3$ Hz, $J3 = 2.0$ Hz, *syn*-allylic H); 5.51 (dd, 1H, $J_1 = 7.9$ Hz, $J_2 = 13.4$ Hz, Hc); 6.6−7.6 (m, 28H, aromatic H).

^{31}P: 13.8 (d, 1P, $J = 41$ Hz); 14.7 (d, 1P, $J = 42$ Hz).

^{13}C{^{1}H}: 15.1; 21.0; 26.0; 65.6; 113.1; 116.3; 116.4; 118.4; 122.2; 122.6; 122.8; 124.1 (d, $J = 6.5$ Hz); 125.5 (d, $J = 6.5$ Hz); 127.4; 128.0; 128.8; 128.9; 129.0; 130.8, 131.0; 131.2; 134.3 (d, $J = 13$ Hz); 135.1; 157.9 (d, $J = 7.9$ Hz).

HR-MS (FAB): $C_{41}H_{37}OP_2Pd^+$ requires 713.1354, found 713.1373.

(C_5H_9)Pd(Xantphos)OTf (6). ^{1}H: 0.9 (t, 3H, $J_1 = J_2 = 8.6$ Hz, *syn*-CH_3); 1.04 (t, 3H, $J_1 = J_2 = 5.7$ Hz, *anti*-CH_3); 1.4−1.9 (br, 6H, ligand CH_3's); 2.74 (br, 1H, *anti*-allylic H); 3.5 (br, 1H, syn allylic H); 5.70 (t, 1H, $J_1 = J_2 = 10.4$ Hz); 6.67 (t, 2H, $J_1 = J_2 = 7.9$ Hz); 7.0−7.6 (br m, 22H, aromatic H); 7.64 (d, 2H, $J = 7.6$ Hz).

^{31}P: 5.3 (br, 1P); 10.4 (br, 1P).

^{13}C{^{1}H}: 36.0; 116.0; 116.3; 116.4; 118.8; 123.8; 123.9; 124.6; 124.7; 127.8; 128.8; 129.0; 130.6; 131.7; 132.7; 134.0; 135.4.

HR-MS (FAB): $C_{44}H_{41}O_2Pd^+$ requires 753.1667, found 753.1685.

(C_3H_5)Pd(Xantphos)BF_4 (7). ^{1}H: 1.54 (s, 3H, ligand-CH_3); 1.81 (s, 3H, ligand-CH_3); 3.5 (m, 2H, *anti*-allylic H); 3.8 (m, 2H, *syn*-allylic H); 6.0 (m, 1H, central allylic H); 6.6 (br t, 2H, Ar−H); 7.0−7.5 (br m, 22H, aromatic H); 7.63 (d, $J = 7.8$ Hz, 2H, aromatic H).

^{31}P: 4.3 (s).

^{13}C{^{1}H}: 25.9; 30.1; 36.3; 118.0; 118.0; 123.1; 125.0; 128.4; 129.3; 130.9; 132.3; 132.7; 133.2; 134.4; 155.2.

HR-MS (FAB): $C_{42}H_{37}OP_2Pd^+$ requires 725.1354 g/mol, found 725.1365 g/mol.

Scheme 9. Determination of the Cone Angle and the Solid Angle, D = Dummy Atom

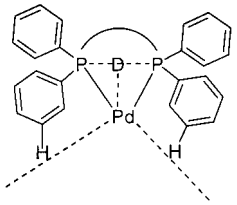

Calculation of Cone Angle and Solid Angle. In the crystal structures, the allyl moiety was removed and a dummy atom was placed in the center of the P−P axis at a nonfixed distance to palladium. The two-dimensional cone angle in the P−Pd−P plane has been calculated viewed from the palladium atom in the direction of the dummy atom. The values thus found for the ligands are listed in Table 6. In all cases, the ligand has a cone angle larger than 180°. The value found for dppe is the smallest (224.6°) and increases for ligands with a larger bite angle to 246.9° for the Xantphos ligand.

A direct comparison between the different ligands is hampered by the fact that some atoms of the phenyl rings of the ligand can be located slightly below or above the P−Pd−P plane. Since these atoms are not taken into account by the two-dimensional cone angle θ, we calculated the three-dimensional solid angle Ω of these ligands in an analogous manner (see Scheme 9). The ligand is again viewed from the palladium atom in the direction of the dummy atom. The solid angle is then determined as a three-dimensional cone angle. The values listed in Table 6 represent the space that the ligands occupy after projection on the central metal atom. The thus determined value for the size of the ligand appears to be dependent on the bite angle of the ligand and increases when the bite angle is larger. Again, the smallest value is found for dppe (4.47 sr) and the largest is found for Xantphos (5.56 sr). The

relatively large value found for the dppf ligand is mainly due to the presence of the large ferrocene unit at a short distance to palladium.

Crystal Structure Determination. Data (Table 7) were collected on an Enraf-Nonius CAD-4 diffractometer with graphite-monochromated Cu Kα radiation and an $\omega-2\theta$ scan. Corrections for Lorentz and polarization effects were applied.

Absorption correction was performed with the program PLATON,[20] following the method of North et al. using Ψ-scans of five reflections for all four compounds.[21] The structures were solved by the PATTY option of the DIRDIF96 program system.[22] The hydrogen atoms were calculated. Full-matrix least-squares refinement was carried out on *F*, anisotropic for the non-hydrogen atoms and isotropic for the hydrogen atoms, restraining the latter in such a way that the distance to their carrier remained constant at approximately 1.0 Å. Scattering factors were taken from Cromer and Mann,[23] *International Tables for X-ray Crystallography*.[24] Anomalous scattering was taken into account.[25] All calculations were performed with XTAL,[26] unless stated otherwise. For **4** the BF_4^- moiety was kept fixed at ideal geometry with isotropic temperature factors $U = 0.15$ Å^2 for B and $U = 0.25$ Å^2 for F; the hydrogen atoms were kept fixed at their calculated positions with $U = 0.10$ Å^2. **5** showed some disorder, which was dealt with in the following way: C(2) was divided over two half-occupied positions, and all H atoms connected to atoms C(1)−C(5) were kept fixed at their calculated positions with $U = 0.10$ Å^2; the BF_4^- moiety also showed disorder, and all F atoms were divided over three $^1/_3$-occupied positions, were kept restrained geometrically to values from literature, and were refined isotropically. After refinement some residual electron density was found in a ΔF synthesis. It was impossible to interpret this density, so it was decided to correct for it by using the option SQUEEZE in the program package PLATON.[20,27] For compound **7** BF_4^- was refined isotropically; the solvent molecule consists of two half-occupied molecules which share their Cl atoms through the center of symmetry; the solvent molecule was refined isotropically, and the H atoms of the solvent were kept fixed with $U = 0.10$ Å^2; the remainder of the H atoms were restrained with fixed temperature factors $U = 0.10$ Å^2.

Acknowledgment. This research was carried out with financial support from DSM Research B.V. and with a subsidy from the Min. Economische Zaken as part of the EET program for clean chemistry.

Supporting Information Available: X-ray crystallographic files in CIF format for the structure determinations of complexes **1**, **4**, **5**, and **7**. This material is available free of charge via the Internet at http://pubs.acs.org.

IC0009167

(20) Spek, A. L. *Acta Crystallogr.* **1990**, *A46*, C34.
(21) North, A. C. T.; Phillips, D. C.; Scott Mathews, F. *Acta Crystallogr.* **1968**, *A26*, 351−359.
(22) Beurskens, P. T.; Beurskens, G.; Bosman, W. P.; de Gelder, R.; Garcia-Granda, S.; Gould, R. O.; Israel, R.; Smits, J. M. M. *The DIRDIF-96 program system*; Crystallography Laboratory, University of Nijmegen: Nijmegen, The Netherlands, 1996.
(23) Cromer, D. T.; Mann, J. B. *Acta Crystallogr.* **1968**, *A24*, 321−324.
(24) Cromer, D. T.; Mann, J. B. *International Tables for X-ray Crystallography*; Kynoch Press: Birmingham, 1974; Vol. IV, p 55.
(25) Cromer, D. T.; Liberman, D. *J. Chem. Phys.* **1970**, *53*, 1891.
(26) *XTAL3.4 User's Manual*; Hall, S. R., King, G. S. D., Stewart, J. M., Eds.; University of Western Australia: Lamb, Perth, 1995.
(27) van der Sluis, P.; Spek, A. L. *Acta Crystallogr.* **1990**, *A46*, 194−201.